Mud bank colonization by opportunistic mangroves: A case study from French Guiana using lidar data

Christophe Proisy, Nicolas Gratiot, E. J. Anthony, Antoine Gardel, François Fromard, Patrick Heuret

HAL Id: halsde-00374860

https://hal.science/halsde-00374860

Mud bank colonization by opportunistic mangroves: A case study from French Guiana using lidar data

Christophe Proisy [a,*], Nicolas Gratiot [b], Edward J. Anthony [c], Antoine Gardel [c], François Fromard [d], Patrick Heuret [e]

[a] *Institut de Recherche pour le Développement (IRD), UMR AMAP, Boulevard de la Lironde, TA-A51/PS2, Montpellier Cedex 5, F-34398 France*
[b] *IRD, LTHE, 1025, rue de la piscine, BP 53, Grenoble F-38041 France*
[c] *Coastal Geomorphology and Shoreline Management Unit (GéoDAL), Université du Littoral Côte d'Opale, MREI 2, 189a Avenue Maurice Schumann, Dunkerque F-59140 France*
[d] *Centre National de la Recherche Scientifique, UMR ECOLAB, 29 rue Jeanne Marvig, BP 4349, Toulouse Cedex 4, F-31055 France*
[e] *Institut National de la Recherche Agronomique (INRA), UMR AMAP, Boulevard de la Lironde, TA-A51/PS2, Montpellier Cedex 5, F-34398 France*

ABSTRACT

Keywords:
Avicennia germinans
Mud crack
Desiccation
Topography
Coastal mud bank
Lidar

Mud bank colonization by mangroves on the Amazon-influenced coast of French Guiana was studied using light detection and ranging (lidar) data which provide unique information on canopy geometry an sub-canopy topography. The role of topography was assessed through analysis of vegetation characteristics derived from these data. Measurements and analyses of mangrove expansion rates over space and time led to the identification of two distinct colonization processes. The first involves regular step-by-step mangrove expansion to the northwest of the experimental site. The second is qualified as 'opportunistic' since it involves a clear relationship between specific ecological characteristics of pioneer *Avicennia* and mud cracks affecting the mud bank surface and for which probabilities of occurrence were computed from terrain elevations. It is argued from an original analysis of the latter relationship that mud cracks cannot be solely viewed as water stress features that reflect desiccation potentially harmful to plant growth. Indeed, our results tend to demonstrate that they significantly enhance the propensity for mangroves to anchor and take root, thus leading to the colonization of tens of hectares in a few days. The limits and potential of lidar data are discussed with reference to the study of muddy coasts. Finally, the findings of the study are reconsidered within the context of a better understanding of both topography and vegetation characteristics on mangrove-fringed muddy coasts.

1. Introduction

Mud in the coastal tropics is often associated with luxuriant mangroves (Saenger, 2003). This is especially the case of the 1600 km-long muddy coast of the Guianas, from Brazil to Venezuela (Fig. 1), where seafront mangroves often attain a height of 40 m and a trunk diameter of 120 cm (e.g. Fromard et al., 1998). Paradoxically, this coast also provides one of the most dramatically changing examples of mud–vegetation interfaces (e.g. Baltzer et al., 2004). Successive erosion and accretion phases due to the drift of mud banks up to 40-km long from the Amazon River to the Orinoco River continuously reshape the physiognomy of the mangrove-fringed coast (e.g. Allison and Lee, 2004). During erosion phases corresponding to 'inter-bank' phases, mangroves are destroyed (e.g. Fromard et al., 1998) whereas during 'bank' phases characterized by mud accretion, the mangrove area increases (Fromard et al., 2004; Gardel and Gratiot, 2006; Gratiot et al., 2007). Perhaps most significantly, an exceptional feature of this coast is that the highest rates of mud bank migration, which attain up to 3 km per year (Gardel and Gratiot, 2005), do not seem to be a handicap to mangrove regeneration in areas subjected to erosion: hundreds of hectares of muddy coast will be rapidly colonized after the beginning of a new bank phase. Also intriguing are the observations from repetitive field campaigns at the same sites, of nearly instantaneous mangrove germination over tens of hectares. Whenever this phenomenon occurs, the entire colonized area exhibits mud cracks.

Many of the experiments carried out on sediment transport and biogeochemical processes along this coast (e.g. special issue of Marine Geology, volume 208, issue 2–4) were restricted to small areas and were not repeated at the same locations because of the difficulties involved in accessing such a soft and flooded environment. Elevation profiles of several hectometres are the very most that can be feasibly achieved during ground surveys

* Corresponding author. Tel.: +33 467 617 545; fax: +33 467 615 668.
  E-mail addresses: christophe.proisy@mpl.ird.fr (C. Proisy), nicolas.gratiot@hmg.inpg.fr (N. Gratiot), edward.anthony@univ-littoral.fr (E.J. Anthony), antoine.gardel@univ-littoral.fr (A. Gardel), francois.fromard@cict.fr (F. Fromard), patrick.heuret@cirad.fr (P. Heuret).
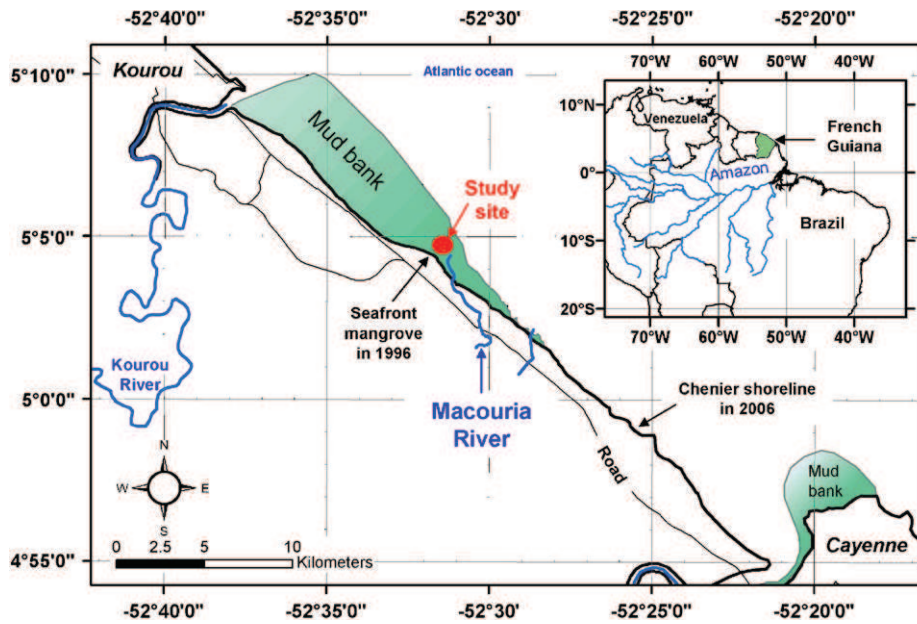
Fig. 1. Location of the study site.

(Lefebvre et al., 2004). The corresponding spatial scale of measurement is insufficient to fully capture the coastal dynamics since mud mobilization and mangrove colonization processes entail large spatio-temporal scales and thus require topographic measurements over large areas and with a resolution on the order of 10 cm (e.g. Lara and Cohen, 2006). Such a degree of accuracy is required because elevation differences of a few centimetres can cause different flooding durations which in turn govern mangrove establishment (e.g. McKee, 1995; Kitaya et al., 2002; Lefebvre et al., 2004; Fiot and Gratiot, 2006).

Although the intertidal bathymetry of mud banks can be mapped using a time series of optical satellite images (Gratiot et al., 2005), the micro-topography of the mud surface cannot be measured with this kind of data. Indeed, monitoring mangrove expansion from satellite images remains qualitative (e.g. Panapitukkul, et al., 1998; Fromard et al., 2004). For example, fine spatial resolution of typically 1 m and additional spectral bands are required to clearly discriminate algal mat response from mangrove tree signatures (e.g. Kutser et al., 2006). Moreover, as imaging sensors only provide 2D information, vegetation height remains difficult to measure from image analysis (e.g. Proisy et al., 2007). It is nonetheless a fundamental parameter related to vegetation growth. For example, spatial observations of mangrove height may highlight when a mud area was colonized provided that mangrove growth is estimated. As demonstrated by Rosso et al. (2006) and Anthony et al. (2007), emerging remote sensing techniques based on lidar (light detection and ranging) may significantly help in studies of intertidal muddy environments. Lidar data can indeed provide simultaneous and detailed information on topography and 3D vertical as well as spatial distribution of forest canopy structure (e.g. Kimes et al., 2006).

The aim of this paper is to assess the interplay between mud bank micro-topography and mud bank colonization by *Avicennia germinans*. From lidar data acquired over 230 ha of a major Amazon-derived mud bank located in French Guiana, both a digital elevation model (DEM) of the mud surface and a digital canopy height model (DCHM) have been generated. By assuming a constant annual growth of young *Avicennia* trees, a spatio-temporal analysis has been carried out both to reconstruct the mangrove expansion history over time and to associate temporal probabilities of mud crack formation. The paper also discusses the

technical limitations of lidar measurements over mangrove-fringed coasts, and the implications of better characterization of mud-vegetation interface in pristine and imperilled or managed mangrove-fringed coasts.

## 2. Study area and data collection

The experimental site is the Macouria mud bank located 5°4′N and 52°32′W, 20 km northwest of Cayenne in French Guiana (Fig. 1). This mud bank has been described in several studies (Gardel and Gratiot, 2005; Fiot and Gratiot, 2006; Gratiot et al., 2007; Anthony et al., 2007), and only aspects of interest to the present work are reported here.

2.1. Changes on the Macouria bank

The leading edge of the Macouria mud bank was singled out as an experimental site in 1996 after an erosion phase that spared the southern part of the area which always consists of a mature mangrove forest (Fig. 2a). Colonization by *A. germinans* west of the Macouria River occurred between October 2001 and August 2002 (Fig. 2b). Mud east of this river underwent widespread colonization. One year later, in August 2003, the colonization front had progressed both east of the river and north-westward (Fig. 2c). A high infrared response over this period suggests the presence of pioneer vegetation on linear bar-like features formed seaward of the main colonized zone. In 2005, the area had almost completely been colonized as clearly observed on the aerial photograph (Fig. 2d). A Spot image of April 2006 confirms the spread of colonization to the northwest, but shows that the mangrove front had not progressed in the seaward direction (Fig. 2e). The trailing edge of the bank reached the experimental site position in 2006, heralding the beginning of an erosion (inter-bank) phase.

2.2. Tide data

The tide is semidiurnal with a spring range of 2.9 m and a neap range of 0.8 m. Mean water level (MWL) and mean high water level (MHWL) are 2.05 and 2.95 m, respectively, whereas mean
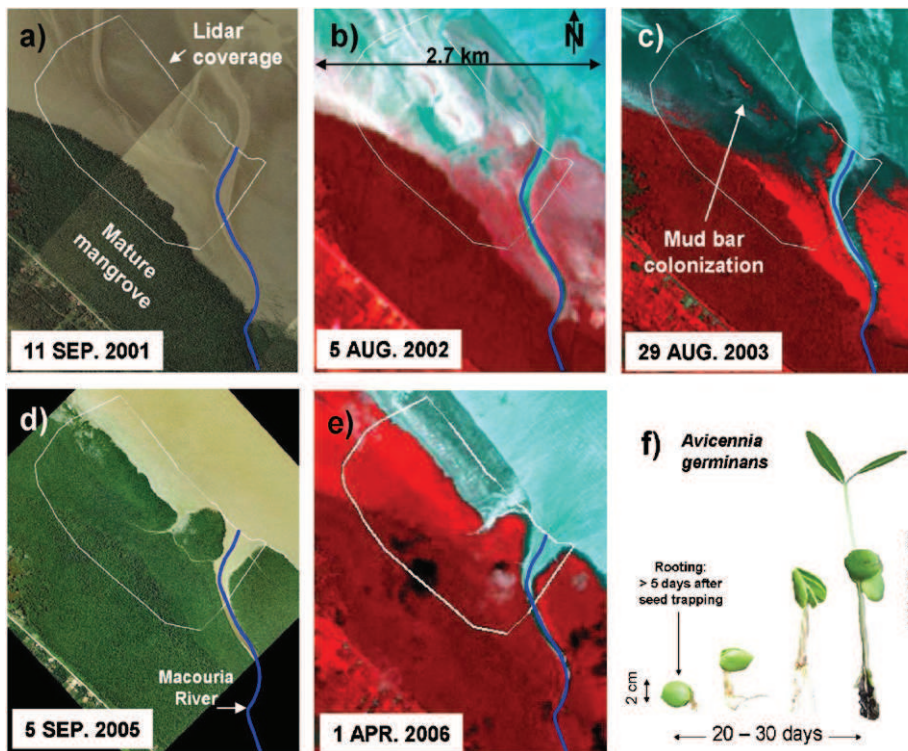
Fig. 2. Temporal evolution of the Macouria experimental site from 2001 to 2006 based on IGN aerial photographs (a, d) and Spot images (b, c, e). The lidar coverage is also indicated. Development of an *A. germinans* seedling (f) (courtesy of M. Herteman).

neap high water level (MNHWL) is 2.6 m (Fiot and Gratiot, 2006). The harmonic components were provided by the Service Hydrographique et Océanographique de la Marine (SHOM: www. shom.fr).

2.3. Basic characteristics of A. germinans trees

As observed in the field, *A. germinans* was undoubtedly the dominant species. In comparison, only few *Laguncularia racemosa* trees were found. In French Guiana, *Rhizophora* spp. is absent during the colonization phase of shoreface-attached mud banks (Fromard et al., 1998). *Avicennia* species have an epigeal germination with cotyledons that expand and are exposed. In French Guiana, seed production is prolific from January to April and decreases towards July (personal observations). With a width of 2 cm, about 5 days are needed for anchoring. Propagules can reach a height of 15 cm in 20–30 days and the first leaves appear in 20–30 days (Fig. 2f). The buoyancy capability of *A. germinans* enables the seeds to float for up to 100 days (Delgado et al., 2001). The majority of both *A. marina* (Australia) and *A. germinans* (Belize, Brazil) often become stranded and establish close to the parent plant population but may be dispersed over greater distances by tidal action, as reported by Clarke (1993) and McKee (1995), respectively.

Growth rates of young *A. germinans* trees are not well known. Within the framework of another study dedicated to the architectural analysis of 2–6 m high *Avicennia* trees, we recorded large disparities in growth rates of more than 50 individuals monitored between December 2003 and April 2005. Maximum values reached 225 cm per year whereas the lowest did not exceed 100 cm per year. Measurements also showed that *Avicennia* trees did not grow regularly through time and that parent generations could be outgrown by their offspring growing nearby (unpublished data). This great disparity was probably due to both changes in local environmental conditions and competition among the trees. As described hereafter, we propose an alternative method of evaluating growth rates of young *Avicennia* trees.

2.4. Lidar data

The lidar data were acquired over a $1.2 \times 2\,km^2$ swath of the Macouria mud bank using the ALTOA system (http://www. altoa.fr/), on October 21, 2004 during a low spring tide. The ALTOA system includes a portable Riegl laser rangefinder (LMS6Q140i-60) embarked on a helicopter flying at a speed of about $30\,m\,s^{-1}$ about 150 m above the ground. The system also consists of two dual-frequency GPS receivers coupled to an inertial navigation system, both systems ensuring that a sub-decimeter differential position can be calculated for the helicopter in post-processing. The rangefinder system is based on the principle of time-of-flight measurement of 30 kHz laser pulses in the infrared wavelength region ($0.9\,\mu m$). As laser beam divergence is 3 milliradians, the footprint is about of 0.22 m wide on the ground. The lidar dataset consisted of a cloud of laser echoes originating from terrain and vegetation. For each point, latitude, longitude and elevation are measured in metres and stored into a file. The datum used is WGS84 and the projection North UTM zone 22.

3. Methods

3.1. Probabilities of mud cracking

According to Fiot and Gratiot (2006), the probability of mud cracks occurring at a given elevation can be estimated from the number of consecutive days of emersion (CDOE). The number of events (NOE) for different CDOEs is computed over a year by comparing the high tide signal to the terrain elevation derived from a lidar-generated elevation model, as described hereafter.
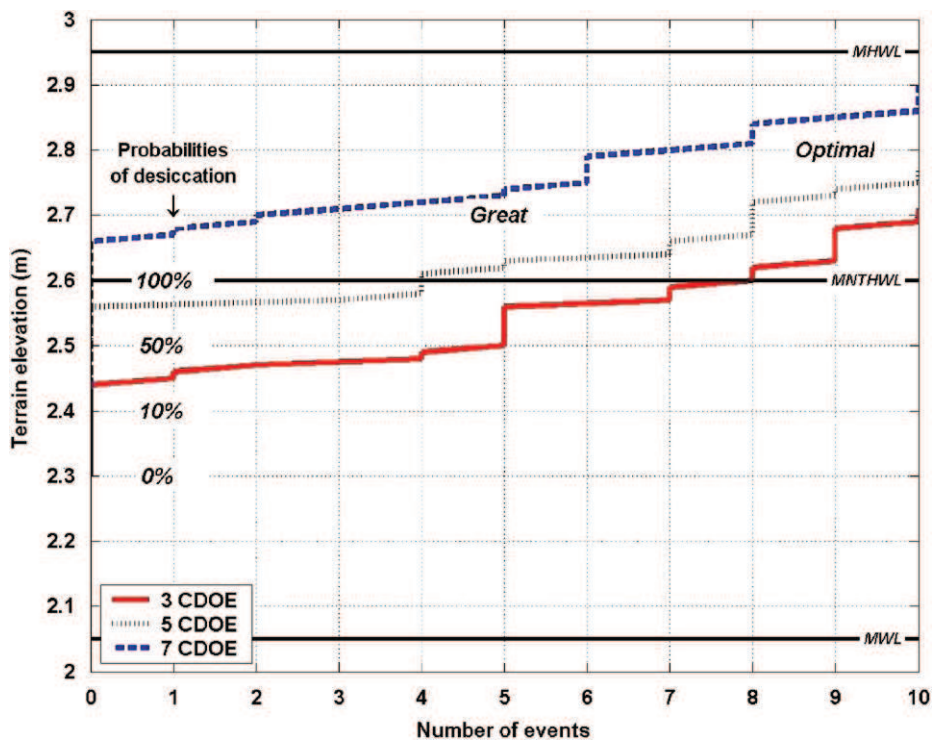
Fig. 3. Statistical distribution of emersion events of a given duration in relation to mud bank elevation (after Fiot and Gratiot, 2006). Emersion periods consist of 3, 5 and 7 consecutive days of emersion (CDOE).

The probability is thus tide-dependent and increases rapidly with terrain elevation, as shown in Fig. 3. For elevations that do not exceed 2.4 m above the hydrographic zero, a single mud crack event has only an estimated 10% chance of developing, whereas this probability reaches 100% when terrain elevation reaches 2.6 m. At elevations of 2.7 m or more, over a period of one year, the durations of emersion and the corresponding number of mud crack events would offer good conditions for *Avicennia* seeds to be trapped. The optimal conditions for seed trapping and colonization are around or below the MHWL. These probabilities are estimated under favorable conditions of drying, and would be reduced to zero under rainy conditions.

3.2. Lidar data processing

3.2.1. DEM computing

A DEM of terrain topography was generated using a kriging interpolation on lowest points and a cell resolution of 2 m (Fig. 4). DEM accuracy is estimated better than 10 cm for elevations over bare areas, whereas it may decrease to 20 cm or more in dense forested areas due to signal interception by the vegetation layer. Dewatering channel networks were digitised from visual DEM interpretation.

For comparisons with the local tide levels, the DEM was calibrated to the hydrographic zero. This was achieved through a calibration transect using a high-resolution total electronic station in March 2003 (Fig. 4; Anthony et al., 2007). Although lidar data were acquired one and a half years later, it was considered that both profiles can be overlaid using the least squares method. This means that we assumed that elevation change during this 18-month period was not significant enough to be measurable within the ± 10 cm of accuracy of the DEM. However, mud deposition probably occurred during this interval but no measurements are available to confirm this. Moreover, mangrove trees are not merely passive colonizers of mud banks. They weaken

currents capable of eroding the sediments and can continuously replenish their environments. Rates of vertical accretion are variable but commonly reach 5 mm per year (e.g. Saenger, 2003).

3.2.2. DCHM computing

Laser echoes from vegetation were separated from those originating from the terrain surface using the DEM as the topographic reference. In other words, points above the DEM value of the corresponding cell were classified as vegetation points, and points below this value taken as echoes from the mud surface. To be confident with this classification, we actually used the DEM cell value plus 25 cm as the real soil-vegetation threshold. Basic statistics on elevation of vegetation-classified points above each DEM cell were then computed and stored in additional raster channels. They included typical statistical data (average, median and maximum, etc). In the following text, we name DCHM the raster with maximum values of laser echoes from vegetation. This lidar-derived product is not shown in a specific figure for reasons of redundancy with the map of germination period described in the following paragraph, as shown later in Fig. 6.

3.2.3. Computing germination periods

During the field experiment in March 2003, it was observed that mangroves had just been established over the mud cape feature indicated in Fig. 4. In October 2004, 19 months later, DCHM-median values over the mud cape yielded a height of about 5.1 m (± 1 m), corresponding to an annual growth rate of 320 cm. A map of germination periods named 'T0M' was derived by computing the ages of colonized cells from their DCHM values. For example, for a cell with a DCHM value of 3.2 m, germination occurred on 21 October, 2003, one year before the lidar flight time and the T0M value was 12 months. Such germination periods should not be taken as exact time frames of the germination process. As explained in the previous section, it should be recalled
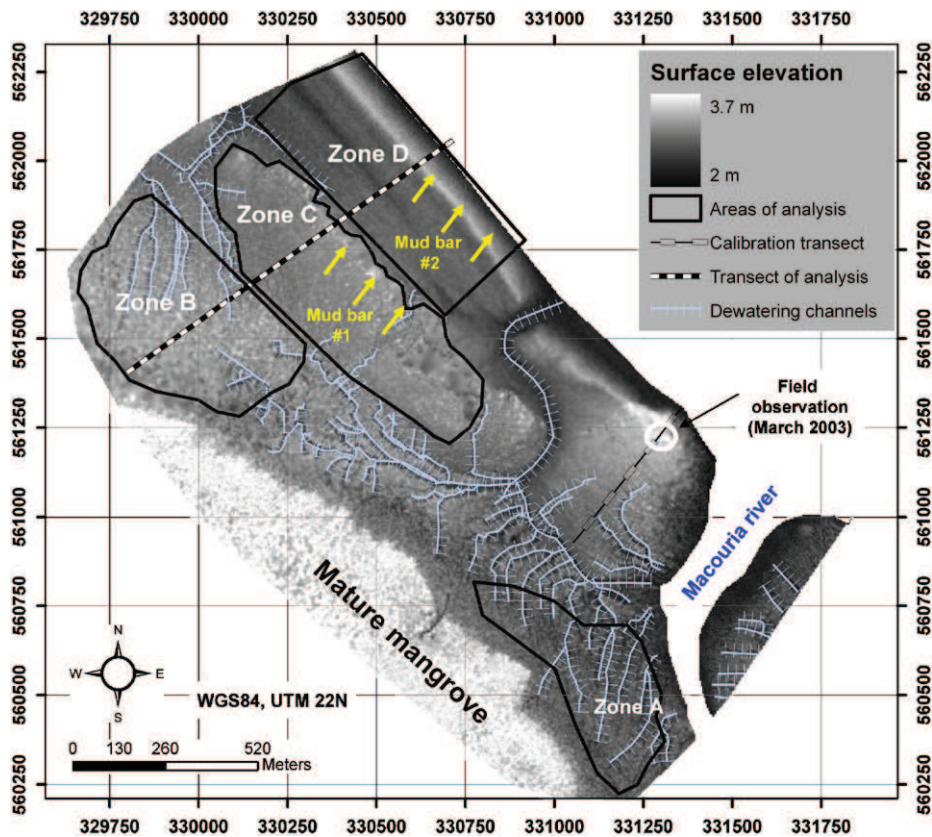
Fig. 4. Lidar-generated DEM. Calibration transect, dewatering channels and observation point are also shown.

that the accuracy of such an age estimation decreases with increasing tree age because of changes in environmental conditions and/or different growth rates throughout the life of any individual tree. The focus is on visualizing how the mud bank surface is spatially colonized time after time, in order to gain a better understanding of the role of topography on the mangrove expansion process.

4. Results

4.1. Mud bank characteristics

4.1.1. Topographic zones

Three major areas of different elevations and hydrologic patterns were discriminated from visual analysis of the DEM (Fig. 4). They were divided into five zones in the following analysis.

The first was the area of mature mangrove which had a significantly higher topographic elevation than the others with a median value of 3.2 m ($\pm$10 cm), i.e. 50 cm above the other mud surfaces. In the following sections, this area is discarded from the analysis since it was not concerned by on-going mangrove colonization.

The second area corresponded to the network of dewatering channels between the old mangrove and the Macouria River. It comprises of two zones, A (13.5 ha) and B (20.5 ha) at about ($\pm$13 cm) and 2.8 m ($\pm$9 cm), respectively (Fig. 5, top graphs). The presence of these drained channels resulted in a rough topographic surface.

In contrast with these drained areas, the third area was mainly characterized by smooth topography. It was located west of the lidar data site between zone B and the sea, but also included the

field measurement site. Although the presence of two 500-m long mud bars was indicated by the bright intensity of the DEM (Fig. 4), the network of dewatering channels had not yet developed. Two zones were delineated in this third area on the basis of their elevation, and named C (25.6 ha) and D (22.6 ha). The frontier between these two zones was taken as the seaward side of the central mud bar, and their median elevations were about 2.7 m ($\pm$7 cm) and 2.6 m ($\pm$14 cm), respectively (Fig. 5, top graphs).

4.1.2. Mangroves in the low tidal zones A and D

Apart from the presence of a topographic high (hereafter named mud bar #2) at the seaward margin of zone D (Figs. 4 and 5, bottom graph), zones A and D were both characterized by the lowest tidal elevations, ranging from 2.5 to 2.6 m. Although they exhibited a similar elevation, these two zones showed contrasting mangrove and soil roughness patterns. Zone A was completely covered by a well-established young mangrove forest (Fig. 5, top graphs; Fig. 6) while zone D was 95% bare (Figs. 5 and 6). Median values of DCHM indicated that vegetation height was about 11 m ($\pm$2 m) for zone A. DCHM values for zone D indicated a very meagre vegetation signal, and only mud bar #2 showed the presence of vegetation, but with a height that did not exceed 40 cm (Fig. 5).

At the elevations of zones A and D, the probability of occurrence of a mud crack event varies from 50% to 100% (Fig. 3). The presence of mangroves in zone A suggests that mud elevation was not the only factor controlling mangrove establishment. This presence moderates the claim by Fiot and Gratiot (2006) of the possible existence of a topographic elevation threshold of about 2.4 m below which mangrove cannot take hold. Such differences in mangrove coverage may be explained by the local geomorphic history (Fig. 1). This suggests that the western river bank (zone A) was sheltered due to both
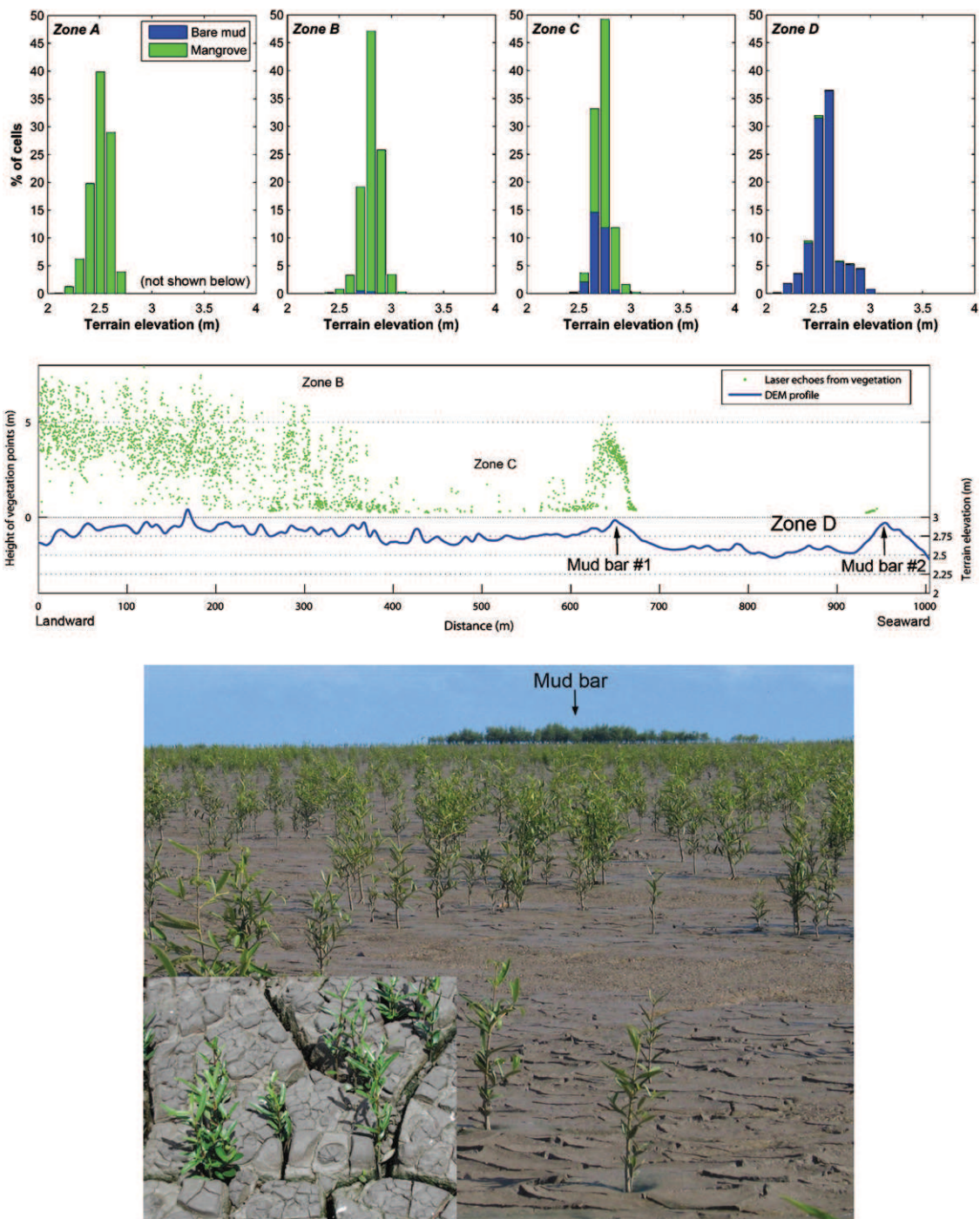
Fig. 5. Percentages of bare mud surface versus colonized mud surface for the four zones A, B, C and D (top graph). Laser echoes from vegetation and DEM values along the transect of analysis across zones B, C and D (middle graph). Illustration of mud cracking over tens of hectares colonized by even-aged *Avicennia* trees, 7 October, 2004, 3 km north of the study site, Macouria bank. The primary phase of colonization, i.e. the tallest trees, is observed on the elongated mud bar at about 600 m in the seaward direction.

consolidation of the eastern part of the mud bank and proximity to the river channel. In contrast, the sea-exposed and bare zone D was formed more recently, and the action of tidal currents and dampened waves is suggested by the smooth topography of this seaward zone. It is to be noted that this zone has remained uncolonized up to 2006 (Fig. 1).

4.1.3. Mangroves in intermediate and high tidal zones B and C

Contiguous zones B and C exhibited intermediate terrain elevations ranging from 2.7 to 2.8 m (Fig. 5). Mangrove trees were uniformly distributed across zone B (Fig. 6), i.e., up to a distance of 400 m from the starting point of the transect profile (Fig. 5, bottom graph). This latter area showed a decrease in vegetation height from 7 to 3 m and exhibited a rough topography mainly due to the network of dewatering channels. A strongly contrasting colonization pattern was observed in zone C between 400 to 680 m where transect of analysis indicated a smooth soil surface (Fig. 5, bottom graph). Colonization was sparse and characterized by scrubby mangroves not exceeding 2.5 m high, while at a distance of 650 m on mud bar #1, mangrove density increased significantly with tree heights of up to 5 m. The surface
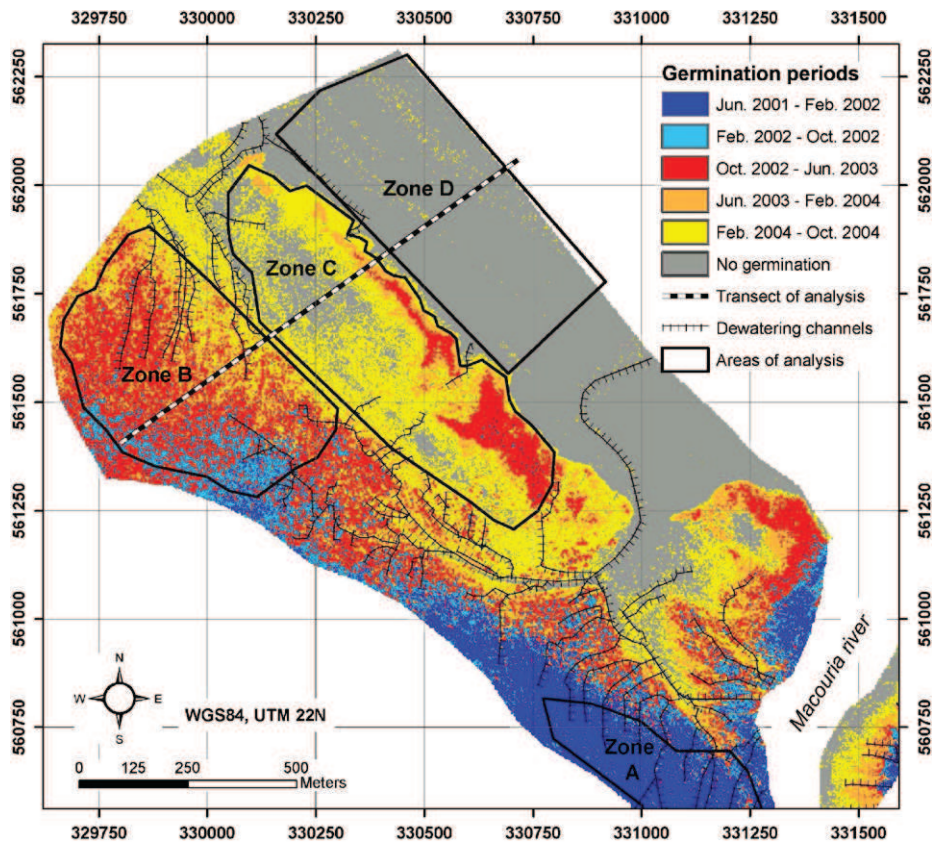
Fig. 6. Lidar-generated map of germination periods named 'T0M' (the mature mangrove area is excluded) using a growth constant of 3.2 m per year.

of this latter zone was relatively smooth in comparison with zone B (Fig. 5, bottom graph). Terrain elevation exhibited a slight decrease from mud bar #1 (2.9 m) to the junction with C zone (2.6 m). Given only surface roughness and DCHM, it is difficult to interpret such differences in mangrove expansion over identical elevation ranges, especially since conditions for mud crack formation in both zones were deemed to be excellent, ranging from 100% to optimal (Fig. 3). It is therefore necessary to analyse the temporal aspects of mud bank colonization. This is carried out in the following section.

4.2. Mud bank colonization

The T0M map and temporal evolution of the number of CDOE events from October 2002 to October 2003 were computed (Figs. 6 and 7, respectively). For reasons of consistency, germination periods of equal duration (8 months), were used to display the colonization process from June 2001 to October 2004. Visualization of T0M, mainly characterized by the red colour (from October 2002 to June 2003), enabled discrimination of the mud bar #1 region. This elongated feature was disconnected in space from the rest of the area that was colonized during the same period (also in red). This spatio-temporal distance, corresponding to the dark grey and yellow areas (June 2003–October 2004) reached 400 m. The lidar data analysis enabled detail characterization in comparison to what was merely suspected from the interpretation of the Spot image (Fig. 2c).

4.2.1. Regular step-by-step colonization towards the northwest
The colonization process began with about 21 ha of terrain colonized in 8 months from June 2001 to February 2002 (blue colour, zone A typically) in the vicinity of both the old mangrove

area and the west bank of the Macouria River. Over the next period, from February 2002 to October 2002 (cyan colour), the mangroves progressed by about 14 ha to the northwest. From October 2002 to June 2003 (red colour), colonization further progressed over 28 ha due to this regular spread from the parent area toward the northwest, zone B being a typical example of this pattern. T0M suggested that this type of colonization process could yield high expansion rates since the computation showed a net advance of about 400 m relative to the adult mangrove frontier in the north direction. This colonization pattern mainly followed that of the dewatering channels. From June 2003 to February 2004, mangrove expansion proceeded exclusively from parent areas and gained 28 ha (orange colour). Notable mangrove progradation was also observed on the Macouria River east bank. After February 2004, T0M displayed an important mangrove expansion of about 32 ha (yellow colour). The surface gained was connected to both sources of mangrove seeds, but expansion was not oriented in any particular direction. In October 2004, 61 ha of bare mud still subsisted.

To summarize, the regular northwest colonization is characterized by step-by-step and continuous pioneer mangrove spread from parent areas in a direction parallel to the Chenier coastline shown in Fig. 1. Close to highly reproductive conspecific adults and in sheltered positions, low intertidal areas also have good chances of being colonized. Network channels probably play an important role in the dispersal of buoyant propagules. The northwest colonization process is at the origin of the regular and typical zonation of coastal mangrove formations (e.g. Panapitukkul, et al., 1998; Fromard et al., 2004).

4.2.2. Top-down opportunistic colonization
Pioneer colonization of mud bar #1 occurred from October 2002 to June 2003 at an elevation of 2.9 m. During this period,
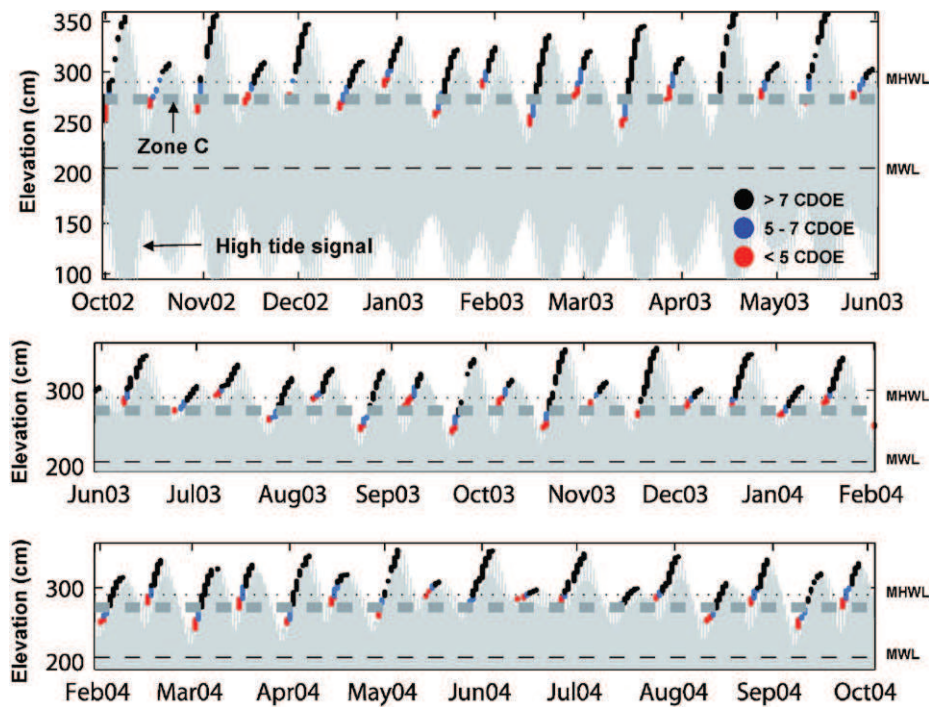
Fig. 7. High tide level and the number of consecutive days of emersion (CDOE) from October 2002 to October 2004. The range 2.7–2.8 m of mud elevation observed in zone C is also shown.

long emersion phases of 5 CDOE at least occurred each month (Fig. 7). As floating *Avicennia* seeds can reach such elevations and need 5 days for anchoring, the probability of germination should become excellent during the large spring tides of February and March, when seed production and chances for mud cracking are at a maximum, i.e., above 7 CDOE (Fig. 7).

Once established in this forward position, mangroves can spread around as observed from June 2003 to February 2004. Although mangrove progression was mainly confined to the mud bar #1 area, colonization spots were observed between this elongated topographic high and the network of dewatering channels (dark grey colour). This area had a median elevation of 2.7 m, i.e. close to the threshold of significant chances of mud crack formation.

From February to October 2004, as stated above, the colonized area (in yellow) was important and linked both regions of propagule dispersion. With a constant growth of 320 cm, we measured an expansion rate reaching 45 ha per year in zone C, whereas the maximum value measured in zone B (regular colonization) did not exceed 20 ha per year. For information purposes, it is worth noting that with an annual growth limited to 150 cm, expansion rates reach 25 and 10 ha per year, respectively.

Mangrove expansion rate cannot increase twofold without the contribution of a typical and visible event that strongly enhances seed trapping. We postulate that this is not a biological event, but rather a physical event related to the mud surface, i.e., the extensive formation of mud cracks in the area of intermediate elevation represented by zone C. The number of emersion events computed for 2004 indeed shows comfortable conditions for mud cracking and for propagule rooting in February, March, April, May, August and September 2004 (Fig. 7; >5 CDOE).

Consequently, we propose the notion of top-down opportunistic colonization, which involves probabilistic mechanisms of colonization by *A. germinans*. The first mechanism involves mud crack formation at the highest elevations, i.e., elongated mud bars. The second mechanism is probably due to the great number of seeds readily available because of the precocious maturity of

Avicennia trees which can become new parents in less than one year. The third mechanism argues for massive trapping of floating propagules by mud cracks. The fourth mechanism is directly related to the formation of mud bars, which serve as veritable forward positions for mangrove dispersal. The opportunistic colonization is top-down because it is initiated from these topographic highs.

5. Discussion

5.1. Limits and potential of lidar data

Lidar technology supplies information on both micro-topography (DEM) and vegetation height (DCHM) in mud bank areas where in-situ field studies are hampered by substrate instability and rapid change. Although lidar provides suitable data for studying forested surfaces in great detail (e.g. MacMillan et al., 2003), the accuracy of lidar measurement for mapping ground elevation under vegetation canopy needs to be better determined (Silvan-Cardenas and Wang, 2006; Rosso et al., 2006). Various filtering techniques enable classification of the point cloud into terrain and vegetation points just on the basis of the spatial relationship of the 3D data (Sithole and Vosselman, 2004). Once the terrain hits are correctly classified, the generation of a DEM is rather straightforward using spatial interpolation methods (Fortin and Dale, 2005). New generations of full-wave lidar instruments may improve both terrain-vegetation classifications and the accuracy of DEMs and DCHMs (e.g. Wagner et al., 2006).

In this work, vegetation height was given by DCHM values of the colonized cells. However, determining tree height using lidar data is not so trivial since the waveform response of a forest is not yet fully understood (Gaveau and Hill, 2003; Lefsky et al., 2005) and requires additional theoretical simulations (e.g. Sun and Ranson, 2000; Kimes et al., 2006). Hence, there is a scope for more significant progress from the coupling of 3D physical modeling with 3D architectural description (e.g. using radar measurements,

Castel et al., 2001). In the case of French Guiana mangroves, assessing *Avicennia* tree architecture and growth is a goal that may provide many benefits in apprehending the functional dynamics of coastal mud bank ecosystems. Within this context, although lidar data acquisitions are still expensive, their use, coupled with field surveys and knowledge of the local tidal signal, may yield fundamental data on the functional attributes of mangrove-fringed coasts.

5.2. Learning from mud bank topography

The results reported here highlight the close relationships between the spatial dynamics of mud bank topography and the capability of mangrove establishment. This work has shown that, in French Guiana, *A. germinans* grows between MWL and MHWL. This could be a specific functioning range for the whole *Avicennia* family since Clarke and Myerscough (1993) indicated the same intertidal range for *Avicennia marina* in southeastern Australia. The present study is a significant contribution to the understanding of this elevation criterion. The intertidal range of Amazon mud banks can be decomposed into two topographic domains. The lower part stands between MWL and MNHWL. Mud bank colonization can occur providing that the area is sheltered from currents. In such areas, mangrove expansion is regular (and somewhat inexorable), occurring step by step from the parent area. As stated earlier, this result shows that *Avicennia* may take hold below an elevation threshold of 2.4 m. Our results confirm the absence of mangrove below 2.4 m only for advanced seaward positions, where the hydrodynamic regime results in a smooth mud surface with little potential for mud crack development, and limits the success of buoyant propagule anchoring.

Between MNHWL and MWL, the rate of regular mangrove expansion increases. But, it would seem that this rate is not enough for opportunistic floating of *Avicennia* propagules. In comparison propagules of competing *Laguncularia* species, which may be qualified as 'sinkers' since they loose their buoyancy in a few days, propagules of *A. germinans* are 'floaters'. This therefore increases the chances of long-distance dispersal and stranding in zones of high elevation (Delgado et al., 2001). In contrast, *A. germinans* propagules may have more difficulties becoming established in the lower intertidal zone due to their easy resuspension by tidal currents. As explained by Delgado et al. (2001), the high number of seeds produced is a way of increasing the chances of assuring at least a minimum number of adult individuals per reproductive period, in an ecosystem where edaphic factors are unfavorable for seedlings during their early stage. In French Guiana, their strategy in colonizing the intermediate and upper tidal zones of Amazon mud banks involves three steps: (1) attainment of an elevated position in the seaward direction, i.e., a macroscale linear bar-like feature, (2) rapid development towards maturity and (3) spread of numerous propagules on the back-bar areas behind the elongated topographic high. Within this context, it would be of significant interest to quantify the proportion of propagules that become established on mud bars and that are transported by the ocean from mangroves shoreward of these bars.

5.3. Learning from mud cracks

The present study reinforces the work of Fiot and Gratiot (2006) on the probabilities of mud cracking as a function of terrain elevation and confirms the mechanical role of mud cracks in mangrove propagule trapping. A spatio-temporal analysis of mangrove expansion could not have been achieved if probabilities of desiccation for different topographic elevation had not been computed.

Mud cracks have been considered in the past as water stress features that reflect desiccation potentially harmful to plant growth (e.g. Clarke, 1993; McKee et al., 2004). However, our study has shown that these features play a major role in fostering rapid and extensive mangrove colonization. As observed in the field, they trap opportunistic *Avicennia* seeds and promote rapid propagule anchorage over mud bars by reducing uprooting due to waves or tidal currents. Their formation strongly varies with the tidal signal from year to year (Fig. 7). In French Guiana, this phenomenon is mainly achieved during the equinox tides of spring and autumn which coincide with the period of proliferation of *Avicennia* propagules. Further field work should evaluate the proportion of Avicennia seeds that are actually trapped in ephemeral mud cracks and investigate the differences in propagule dispersal between flooding and dewatering periods.

These mud cracks also constitute a typical example of interplay effects between sediments and mangroves. As pointed out by Anthony et al. (2007) in a study dedicated to the topography of the Macouria bank, long linear wave-formed mud bars may have a fundamental influence in this interplay by providing low-energy back-bar areas where fresh mud is deposited, thus increasing the surface area liable to mud crack formation. If this postulate turns out to be correct, it will provide a valuable explanation of field observations such as those presented in Fig. 5.

5.4. Lessons from pristine coasts

Rehabilitation of imperilled mangrove coasts (e.g. Lewis III, 2005) could also benefit from the hitherto unsuspected role of mud cracks highlighted by our study of pristine mangroves on the Amazon-influenced coast of French Guiana. By providing markers ready to be colonized, mud crack areas can be directly targeted as zones where the chances of successful mangrove replanting aimed at rehabilitation are highest. A simple experimental approach consisting in sowing, from a boat, mangrove seeds over mud crack areas may yield insight into the rehabilitation potential. Although there are numerous types of mangrove forests in a wide variety of topographic settings, such a simple test is a very low-cost one in comparison to tedious manual planting of propagules. Because they are desiccation features, mud cracks are indicative of mud dewatering conditions that can be stressful for vegetation growth. This ambivalent propensity to foster mangrove growth, as in French Guiana, or to reflect environmental conditions that could hinder plant growth, highlights the importance of the relationship between wetting by tidal flooding and mangrove species.

Mangrove establishment on mud banks will depend on biological characteristics such as buoyancy, stomatal conductance, assimilation rate, etc. (e.g. Delgado et al., 2001; Kitaya et al., 2002; Ye et al., 2004). Consequently, in a mangrove rehabilitation programme, the selection of species must be appropriate in order to be able to follow up the impact of topography and the probabilities of desiccation.

5.5. Conclusions

Mangrove sediments have a unique history at any individual site which, when properly apprehended, can provide significant insights into general patterns of mangrove ecosystem functioning (Saenger, 2003). This is the case of Amazon-influenced coasts which offer intriguing mud-vegetation interfaces with a considerable potential for ground-breaking interdisciplinary research. The work reported here has called for interdisciplinary gap-bridging

involving sedimentology, geomorphology, hydrology, mangrove ecology and remote sensing. It is our strong belief that the opportunistic behaviour of Amazon mangroves is hinged on the formation, by waves, of mud bars over mud banks. This may well be the critical factor that explains the strong resilience of French Guiana mangroves in the face of drastic coastal changes induced by mud bank migration from the Amazon to the Caribbean.

References

Allison, M.A., Lee, M.T., 2004. Sediment exchange between Amazon mudbanks and shore-fringing mangroves in French Guiana. Marine Geology 208 (2–4), 169–190.

Anthony, E.J., Dolique, F., Gardel, A., Gratiot, N., Polidori, L., Proisy, C., 2007. Nearshore intertidal topography and topographic-forcing mechanisms of an Amazon-derived mud bank in French Guiana. Continental Shelf Research 28 (6), 813–822.

Baltzer, F., Allison, M., Fromard, F., 2004. Material exchange between the continental shelf and mangrove-fringed coasts with special reference to the Amazon-Guianas coast. Marine Geology 208 (2–4), 115–122.

Castel, T., Beaudoin, A., Floury, N., Le Toan, T., Caraglio, Y., Barczi, J.F., 2001. Deriving forest canopy parameters for backscatter models using the AMAP architectural plant model. IEEE Transactions on Geoscience and Remote Sensing 39 (3), 571–583.

Clarke, P.J., 1993. Dispersal of grey mangrovenext term (*Avicennia marina*) propagules in southeastern Australia. Aquatic Botany 45 (2–3), 195–204.

Clarke, P.J., Myerscough, P.J., 1993. The intertidal distribution of te grey mangrove (*Avicennia marina*) in southeastern Australia: the effects of physical conditions, interspecific competition, and predation on propagule establishment and survival. Australian Journal of Ecology 18, 307–315.

Delgado, P., Hensel, P.F., Jiménez, J.A., Day, J.W., 2001. The importance of propagule establishment and physical factors in mangrove distributional patterns in a Costa Rican estuary. Aquatic Botany 71 (3), 157–178.

Fiot, J., Gratiot, N., 2006. Structural effects of tidal exposures on mudflats along the French Guiana coast. Marine Geology 228 (1–4), 25–37.

Fortin, M.-J., Dale, M.R.T., 2005. Spatial Analysis: A Guide For Ecologists. Cambridge University Press, Cambridge, UK.

Fromard, F., Puig, H., Mougin, E., Marty, G., Betoulle, J.L., Cadamuro, L., 1998. Structure, above-ground biomass and dynamics of mangrove ecosystems: new data from French Guiana. Oecologia 115, 39–53.

Fromard, F., Vega, C., Proisy, C., 2004. Half a century of dynamic coastal change affecting mangrove shorelines of French Guiana. A case study based on remote sensing data analyses and field surveys. Marine Geology 208 (2–4), 265–280.

Gardel, A., Gratiot, N., 2005. A satellite image-based method for estimating rates of mud bank migration, French Guiana, South America. Journal of Coastal Research 21 (4), 720–728.

Gardel, A., Gratiot, N., 2006. Monitoring of coastal dynamics in French Guiana from 16 years of SPOT satellite images. Journal of Coastal Research (SI 39), 1503–1506.

Gaveau, D.L.A., Hill, R.A., 2003. Quantifying canopy height underestimation by laser pulse penetration in small-footprint airborne laser scanning data. Canadian Journal of Remote Sensing 29 (5), 650–657.

Gratiot, N., Gardel, A., Polidori, L., 2005. Remote sensing based bathymetry on the highly dynamic Amazonian coast. 9th International Coastal Symposium, Hofn, Iceland, 5–8 June 2005. ⟨http://www.icecoast.is/ics2005⟩.

Gratiot, N., Gardel, A., Anthony, E.J., 2007. Trade-wind waves and mud dynamics on the French Guiana coast, South America: input from ERA-40 wave data and field investigations. Marine Geology 236 (1–2), 15–26.

Kimes, D.S., Ranson, K.J., Sun, G., Blair, J.B., 2006. Predicting Lidar measured forest vertical structure from multi-angle spectral data. Remote Sensing of Environment 100 (4), 503–511.

Kitaya, Y., Jintana, V., Piriyayotha, S., Jaijing, D., Yabuki, K., Izutani, S., Nishimiya, A., Iwasaki, M., 2002. Early growth of seven mangrove species planted at different elevations in a Thai estuary. Trees-Structure and Function 16 (2–3), 150–154.

Kutser, T., Vahtmae, E., Martin, G., 2006. Assessing suitability of multispectral satellites for mapping benthic macroalgal cover in turbid coastal waters by means of model simulations. Estuarine, Coastal and Shelf Science 67 (3), 521–529.

Lara, R.N., Cohen, M., 2006. Sediment porewater salinity, inundation frequency and mangrove vegetation height in Bragança, North Brazil: an ecohydrology-based empirical model. Wetlands Ecology and Management 14 (4), 349–358.

Lefebvre, J.P., Dolique, F., Gratiot, N., 2004. Geomorphic evolution of a coastal mudflat under oceanic influences: an example from the dynamic shoreline of French Guiana. Marine Geology 208 (2–4), 191–205.

Lefsky, M.A., Hudak, A.T., Cohen, W.B., Acker, S.A., 2005. Geographic variability in Lidar predictions of forest stand structure in the Pacific Northwest. Remote Sensing of Environment 95 (4), 532–548.

Lewis III, R.R., 2005. Ecological engineering for successful management and restoration of mangrove forests. Ecological Engineering 24 (4), 403–418.

MacMillan, R.A., Martin, T.C., Earle, T.J., McNabb, D.H., 2003. Automated analysis and classification of landforms using high-resolution digital elevation data: applications and issues. Canadian Journal of Remote Sensing 29 (5), 592–606.

McKee, K.L., 1995. Seedling recruitment patterns in a Belizean mangrove forest: effects of establishment ability and physico-chemical factors. Oecologia 101, 448–460.

McKee, K.L., Mendelssohn, I.A., Materne, M.D., 2004. Acute salt marsh dieback in the Mississippi River deltaic plain: a drought-induced phenomenon? Global Ecology and Biogeography 13 (1), 65–73.

Panapitukkul, N., Duarte, C.M., Thampanya, U., Kheowvongsri, P., Srichai, N., Geertz-Hansen, O., Terrados, J., Boromthanarath, S., 1998. Mangrove colonization: mangrove progression over the growing Pak Phanang (SE Thailand) mud flat. Estuarine, Coastal and Shelf Science 47 (1), 51–61.

Proisy, C., Couteron, P., Fromard, F., 2007. Predicting and mapping mangrove biomass from canopy grain analysis using Fourier-based textural ordination of IKONOS images. Remote Sensing of Environment 109 (3), 379–392.

Rosso, P.H., Ustin, S.L., Hastings, A., 2006. Use of Lidar to study changes associated with Spartina invasion in San Francisco Bay marshes. Remote Sensing of Environment 100 (3), 295–306.

Saenger, P., 2003. Mangrove Ecology, Silviculture and Conservation. Kluwer Academic Publishers, Dordrecht, NL.

Silvan-Cardenas, J.L., Wang, L., 2006. A multi-resolution approach for filtering Lidar altimetry data. ISPRS Journal of Photogrammetry and Remote Sensing 61 (1), 11–22.

Sithole, G., Vosselman, G., 2004. Experimental comparison of filter algorithms for bare-Earth extraction from airborne laser scanning point clouds. ISPRS Journal of Photogrammetry and Remote Sensing, Advanced Techniques for Analysis of Geo-spatial Data 59 (1–2), 85–101.

Sun, G.Q., Ranson, K.J., 2000. Modeling Lidar returns from forest canopies. IEEE Transactions on Geoscience and Remote Sensing 38 (6), 2617–2626.

Ye, Y., Tam, N.F.Y., Wong, Y.S., Lu, C.Y., 2004. Does sea level rise influence propagule establishment, early growth and physiology of Kandelia candel and Bruguiera gymnorrhiza? Journal of Experimental Marine Biology and Ecology 306 (2), 197–215.

Wagner, W., Ullrich, A., Ducic, V., Melzer, T., Studnicka, N., 2006. Gaussian decomposition and calibration of a novel small-footprint full-waveform digitising airborne laser scanner. ISPRS Journal of Photogrammetry and Remote Sensing 60 (2), 100–112.